Conditionally-Averaged Structures in Wall-Bounded Turbulent Flows

By Yann G. Guezennec,[1] Ugo Piomelli[2] and John Kim[3]

The quadrant-splitting and the wall-shear detection techniques were used to obtain ensemble-averaged wall layer structures. The two techniques give similar results for Q4 events, but the wall-shear method leads to smearing of the Q2 events. Events were found to maintain their identity for very long times ($\sim 50t^+$). The ensemble-averaged structures scale with outer variables. Turbulence producing events were associated with one dominant vortical structure rather than a pair of counter-rotating structures. An asymmetry-preserving averaging scheme was devised that allowed to obtain a picture of the "average" structure which more closely resembles the instantaneous one.

1. Objectives

It was our goal to study coherent structures found in turbulent channel and boundary layer flows using the direct numerical simulation data bases.

Specifically, the following issues were examined:

- Comparison between the ensemble-averaged structures detected by the quadrant-splitting technique and those obtained by the wall-shear detection scheme.
- Scaling of the size of these ensemble-averaged structures with Reynolds number.
- Tracking of individual events (quadrant detected and wall-shear detected) in time to determine their propagation velocity and their persistence.
- Comparison between the structures obtained by ensemble-averaging and those observed instantaneously in the flow.
- Design of better detection and averaging procedures to yield average structures more representative of the instantaneous ones.

2. Procedure

Most of the present results were obtained from the direct numerical simulation of a turbulent channel flow at a Reynolds number $Re_\tau = 180$ based on channel halfwidth δ and friction velocity (Kim, Moin and Moser, 1987). Some additional results were also obtained from the direct numerical simulation of a turbulent boundary layer at $Re_\theta = 670$ based on momentum thickness θ and friction velocity (Spalart, 1987).

1 Ohio State University
2 Stanford University
3 NASA-Ames Research Center

Coherent structures, defined here as large contributors to the turbulence production process, were detected using two techniques. The first one was the quadrant-splitting technique, which identified events characterized by a fluctuating Reynolds stress larger than 3.5 times the product of the long-term r.m.s. of the streamwise (u') and normal (v') velocity fluctuations. The detection was performed at $y^+ = 12$ and events were sorted into second (Q2) and fourth (Q4) quadrant in the usual manner.

The second detection technique was the wall-shear technique used experimentally by Nagib and Guezennec (1986). With this technique, Q4 events were detected whenever the fluctuating instantaneous wall stress $\tau'_{12} \sim \partial u'/\partial y|_w$ exceeded its r.m.s. intensity by more than 2.8 times while the spanwise shear $\tau'_{32} \sim \partial w'/\partial y|_w$ was small (less than half its r.m.s. intensity). Q2 events were detected in a similar fashion when $-\tau'_{12}$ was over 1.8 times its r.m.s. value. The difference in threshold values for the Q2 and Q4 events was necessary to detect a similar number of events and is consistent with the positive skewness of the wall shear probability distribution.

For both techniques, centering in the streamwise (x) and spanwise (z) direction was performed whenever several neighboring points met the detection criteria by selecting only the one at which the perturbation was maximum. Ensemble averages of the three velocity components were performed for each type of event and detection technique. An average of 100 events were detected with each scheme for the channel flow data, and 500 for the boundary layer data (due to the larger spatial extent of the computational box). Results of the ensemble-averaging procedure were examined by vector maps in various cross-cuts through the events.

3. Results

3.1 Validation of wall-shear detection technique

Results obtained with the two detection technique were compared in the channel flow case. Figure 1 shows such a comparison for a streamwise cut through the centerline of the Q4 event. The two techniques yield essentially the same result. Comparisons were also performed for various spanwise cuts (not shown here) and confirmed this result. Figure 2 represents a similar comparison for the Q2 event. Although the patterns are qualitatively the same, the quadrant splitting technique yields a much more localized perturbation in the streamwise direction. The wall-shear detection technique is not as selective for this type of event, resulting in a lack of registration in the streamwise direction. This is consistent with the fact that the Q2 events represent motion away from the wall, and are less detectable by their imprint on the wall than the Q4 events. However, spanwise cross-cuts (not shown here) are quite similar with both techniques, indicative of little smearing in the spanwise direction.

3.2. Scaling of ensemble-averaged structures

The effect of the Reynolds number on the size of the ensemble-averaged structures was then examined. In order to compare with the experimental results of Wark, Nagib and Guezennec (1987), in which only two velocity components were

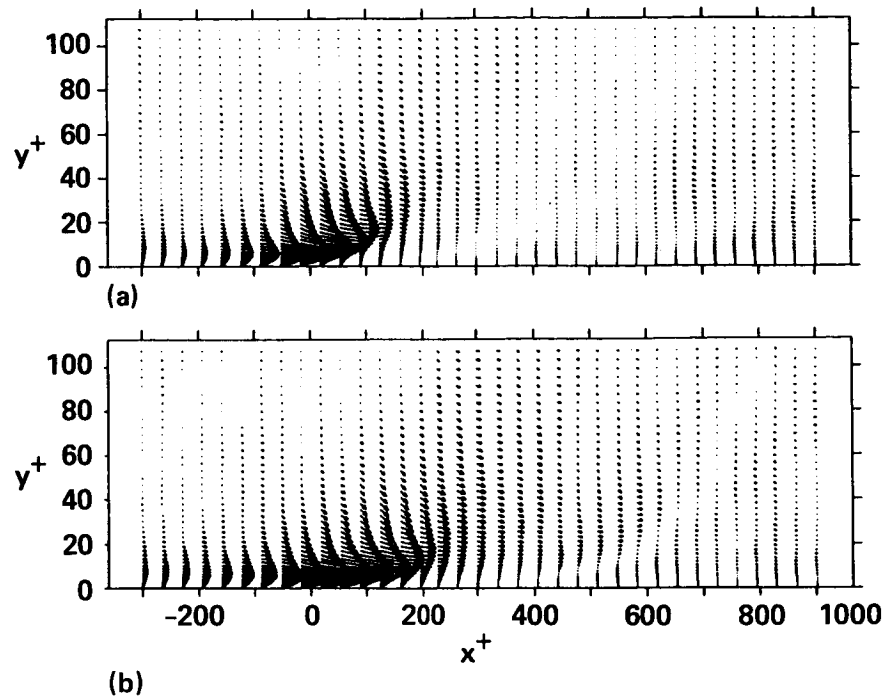

FIGURE 1. Ensemble-averaged perturbation velocity maps of the fourth quadrant events. The maximum velocity fluctuations in figure are approximately equal to $5u_\tau$. (a) Events detected by quadrant splitting technique; (b) events detected by wall shear technique.

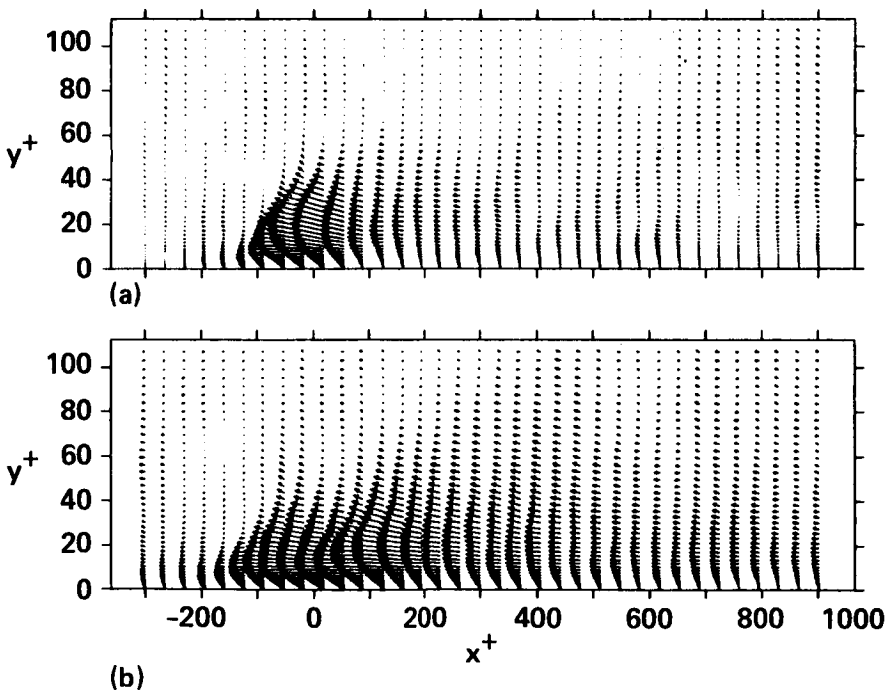

FIGURE 2. Ensemble-averaged perturbation velocity maps of the second quadrant events. The maximum velocity fluctuations in figure are approximately equal to $5u_\tau$. (a) Events detected by quadrant splitting technique; (b) events detected by wall shear technique.

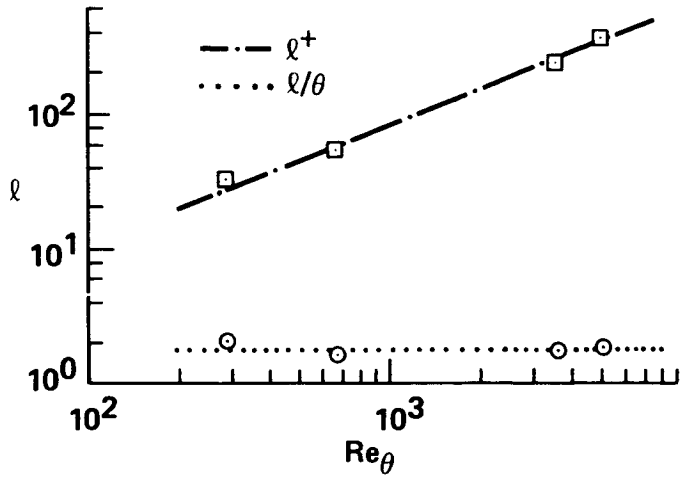

FIGURE 3. Reynolds number dependence of the transverse characteristic scale of the ensemble-averaged structures.

measured, a procedure similar to theirs was used to estimate the characteristic spanwise length scale. At the streamwise location of the detection point, the streamwise velocity perturbation was integrated over the height of the structure to yield a local "perturbation displacement thickness". This procedure was repeated at various spanwise positions. The characteristic spanwise length scale was then arbitrarily chosen as the distance away from the centerline where this perturbation displacement thickness became zero. This distance was checked visually to correspond approximately to the center of the vortical structures detected. This procedure was applied to the events detected by the gradient technique. Q2 and Q4 events also yielded comparable results. Figure 3 shows the variation of this length scale, ℓ, with Reynolds number, Re_θ. The lowest Reynolds number (250) corresponds to the channel flow data and the second point (670) correspond to the boundary layer simulation. The upper two point were determined experimentally by Wark *et al.* (1987). When the size is non-dimensionalized with inner variables (u_τ and ν), it increases with Reynolds number. On the other hand, it remains constant when non-dimensionalized with outer variables (θ) over a twenty-fold increase in Reynolds number.

3.3. Propagation velocity and persistence

Quadrant-type events were tracked in successive time frames to determine their propagation velocity and persistence. Time frames were 3 viscous time units apart, so that the identification and matching of corresponding events in successive time frames was unambiguous. The coordinates of each event were then recorded as a function of time. Events were found to propagate in the streamwise direction with very little meandering in the spanwise direction. Figure 4 illustrates the space-time trajectories of the individual Q2 (top) and Q4 (bottom) events. The average slope of these trajectories represent the propagation velocity of the events and was found

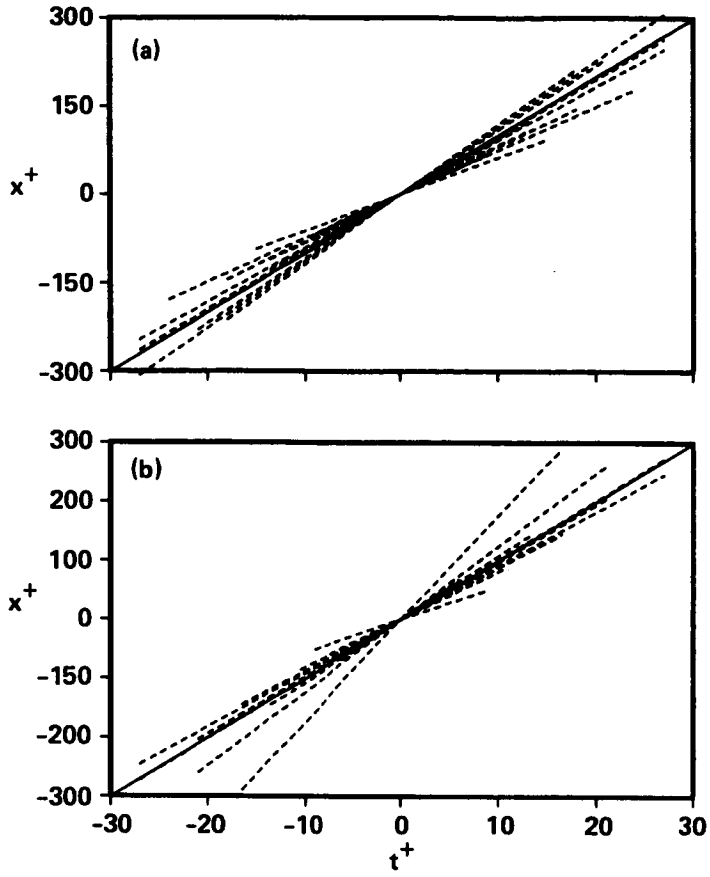

FIGURE 4. Space-time trajectories of events. (a) Second quadrant; (b) fourth quadrant.

to be $9.3u_\tau$ for the Q2-type and $10.3u_\tau$ for the Q4-type events. The local mean velocity at this y-location was $9.5u_\tau$. Moreover, it should be noted that the events maintain their identity for a rather long time (of the order of 40 to 60 viscous time units). This indicates that they do not break up under some rapid instability once they have been formed. The high frequency oscillations observed in laboratory measurements with a fixed probe are linked to their localized spatial extent and propagation velocity. Similar tracking was also performed for wall-shear detected events. They were also found to propagate at similar speeds and persist for similar durations. This finding confirms that large wall-shear fluctuations are the imprint of structures residing in the buffer or logarithmic layer and has important implications for numerical modeling of the wall layer.

3.4. Link between instantaneous and ensemble-averaged structures

Cross-stream vector maps of each individual quadrant event were examined to understand the relation between the instantaneous structures and those obtained from the ensemble-averaging process. While the averaged event resulted in a symmetric pair of counter-rotating vortical structures, due to the homogeneity of the

flow in the spanwise direction, individual realizations differed greatly from this pattern, in terms of size and strength of the structures and, in particular, of symmetry. An example of such difference between the ensemble-averaged pattern and a typical realization is shown in Figure 5. The instantaneous field shows the presence of a strong vortical structure on one side and of a weak one on the other side. Based on this visual evidence, a procedure to measure this asymmetry was designed. Circulation was computed around a closed path (square for simplicity) on each side of the detection point to measure the strength of each vortical structure. Since these structures appear in different sizes, the circulation Γ was computed around four separate integration contours as illustrated in Figure 5b. For each contour the circulation was averaged over both sides and all events to determine the choice of an appropriate contour size. The results are shown in Figure 6 for the Q2 events. The second contour contains the entire structure, and the average circulation Γ_{av} is maximum; along the larger paths the average circulation decreases due to the effect of viscosity. Based on these observations, the second path was chosen and the asymmetry of the event was estimated by the difference $\Delta\Gamma$ of the circulation between the two sides. The normalized probability density function of this measure of asymmetry is shown in Figure 7 as a function of $\Delta\Gamma$ normalized by Γ_{av} (the probability density function was normalized so that its integral is 1 over the whole distribution). This symmetry parameter has a bi-modal distribution, indicating that the most likely event is strongly one-sided, *i.e.* associated with one dominant vortical structure. Similar results were obtained for the Q4 events.

3.5. New ensemble-averaging technique

Based on the result of the previous section, a new ensemble-averaging procedure was designed that recognizes the asymmetry of the individual structures. For each event, the stronger side was identified by the procedure described above and the individual structures were "flipped" about the centerline if necessary, so that the strong structure was always on the same side. The ensemble averaging procedure was then carried out as usual. The comparison between the conventional procedure and this new one is shown in Figure 8 for the Q2 event. The average event is now characterized by only one dominant vortical structure associated with a strong Q2 motion on the centerline. It is worthy to notice the presence of a rather strong Q4 motion on the other side of the structure. This is consistent with the observation that Q4 and Q2 events appear often in pairs side by side. This average structure resembles more closely the individual realizations (there is of course an equal probability of finding its mirror image). The fact that strongly asymmetric structures (or possibly even single structures) are more likely to occur has an important implication on their dynamics. For example, the mutual induction effect for lifting away from the wall commonly used to describe their evolution loses some of its appeal.

4. Conclusions

In summary, the following conclusions have been reached:

- The wall-shear detection technique works well for the fourth quadrant events, but leads to substantial streamwise smearing of the second quadrant events. Events

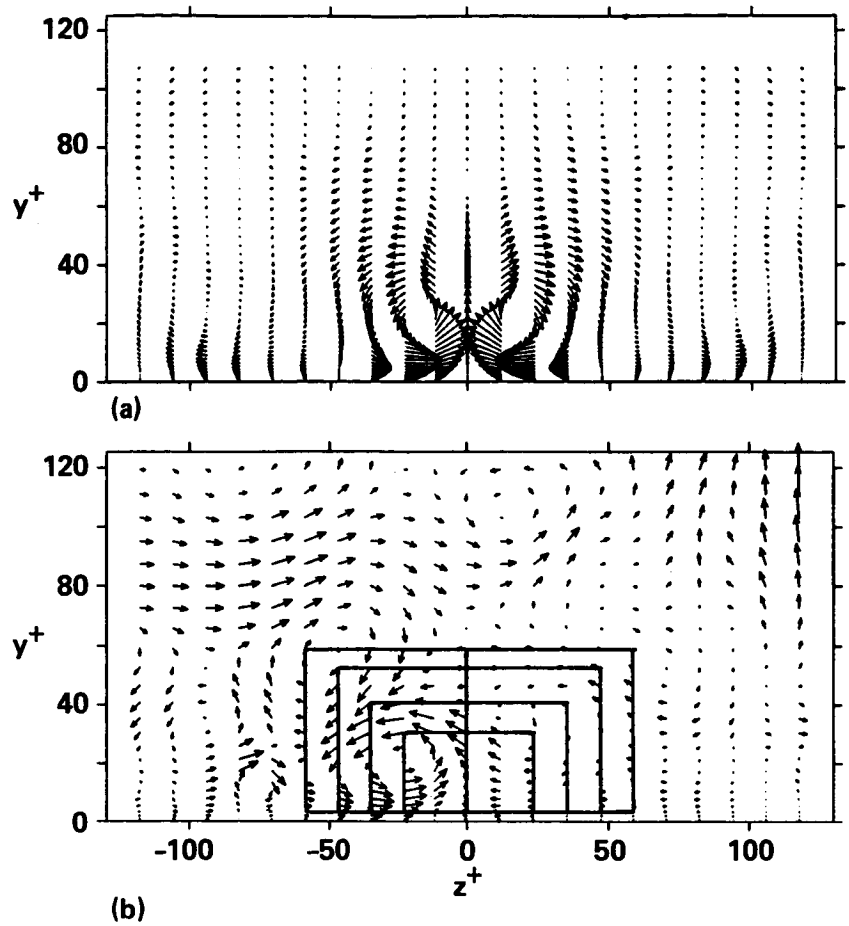

FIGURE 5. Comparison between the ensemble-averaged structure (top) and a typical instantaneous structure of a second quadrant event (bottom), highlighted with circulation integration paths. The maximum velocity fluctuations are approximately equal to u_τ in the top figure and to $2u_\tau$ in the bottom figure.

detected by both techniques have, however, similar spanwise structures.

- Turbulence producing events (regardless of the method of detection, *i.e.* wall-shear, quadrant-splitting or VITA/VISA events, which represent the interaction of two opposite quadrant events) propagate at a speed of approximately $10u_\tau$ in the wall region ($y^+ \leq 15$), with the sweeps being slightly faster than the ejections. They retain their coherence over a period of the order of $50t^+$ and over a streamwise extent of the order of $500\ell^+$. It is therefore unlikely that strong instabilities convected with these structures lead to their catastrophic break up.
- The size of ensemble-averaged structures scales with outer variables, *i.e.* it appears to follow the growth of the logarithmic layer with the Reynolds number. Therefore, they become more and more distinct from the wall layer as the Reynolds number increases. However, it must be noted that this scaling applies to the ensemble-averaged structures, and possibly stems from the fact that a larger

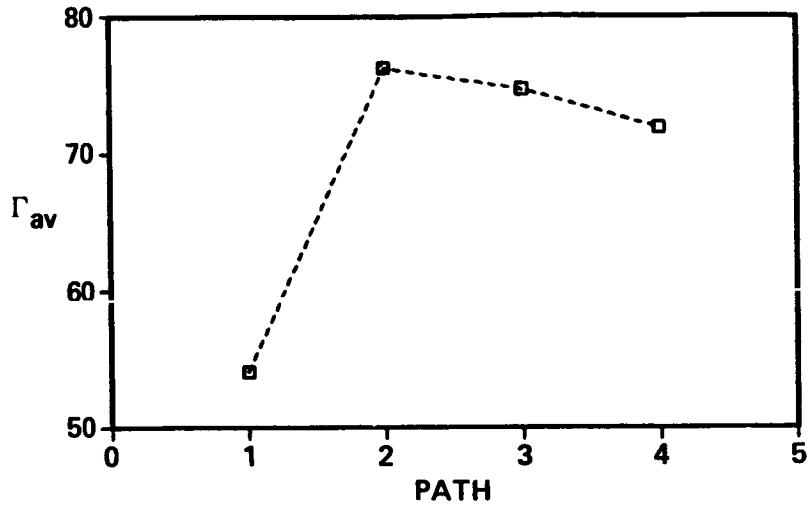

FIGURE 6. Average strength of vortical structures for different integration paths.

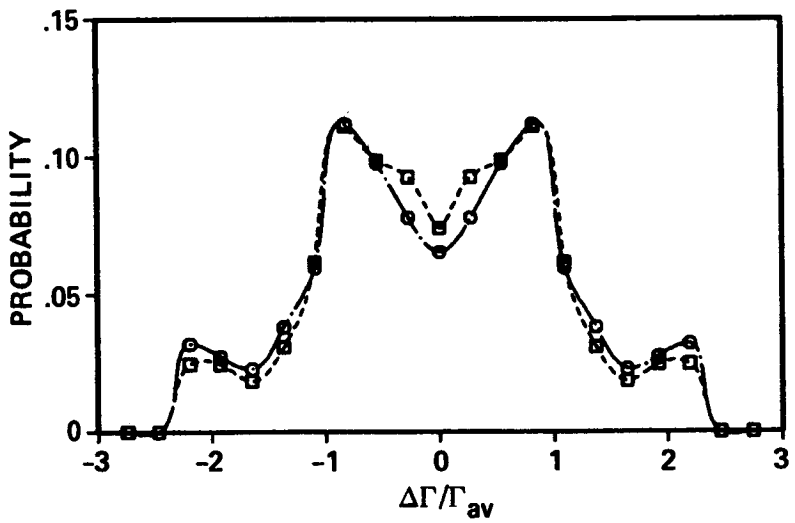

FIGURE 7. Probability density of the asymmetry of vortical structures. Second quadrant event.

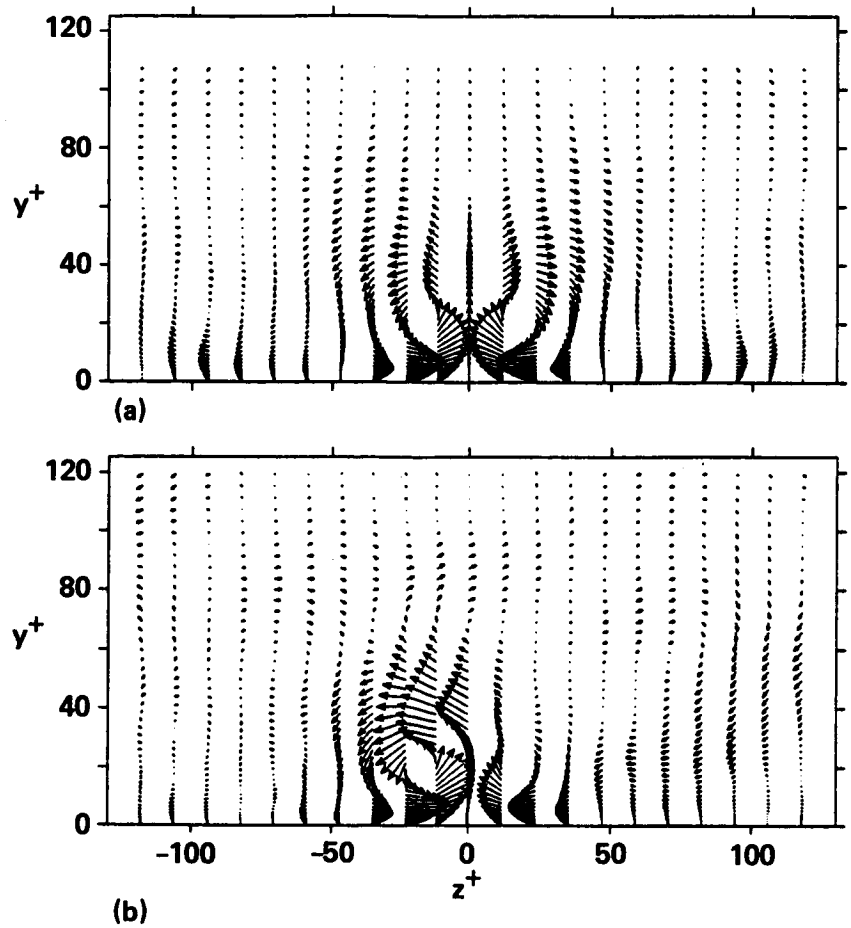

FIGURE 8. FIGURE 8. Ensemble-averaged structures for the second quadrant event. The maximum velocity fluctuations in figure are approximately equal to u_τ. (a) Conventional averaging technique; (b) modified averaging technique.

range of individual sizes exists at higher Reynolds numbers. This indicates the need to perform more high Reynolds number experiments (physical or numerical) to distinguish more clearly the hierarchy of scales associated with the coherent structures.

- Turbulence producing events were found to be associated with one dominant vortical structure rather than a pair of counter-rotating structures. This represents the first step in obtaining "sharper" ensemble averages which are more representative of the instantaneous flow topology. The correct kinematic description of these structures will undoubtedly lead to a better understanding of their dynamics, and more accurate structural information to be incorporated in turbulence models.

REFERENCES

KIM, J., MOIN, P. & MOSER, R. 1987 Turbulence statistics in fully developed channel flow at low Reynolds number. *J. Fluid Mech.*. **177**, 133-160.

NAGIB, H.M. & GUEZENNEC, Y.G. 1986 On the Structure of Turbulent Boundary Layers. Proceedings of the Tenth Symposium on Turbulence, University of Missouri, Rolla.

SPALART, P.R. 1986 Direct Simulation of a Turbulent Boundary Layer up to $Re_\theta = 1410$. NASA T.M.89407.

WARK, C.E., NAGIB, H.M. & GUEZENNEC, Y.G. 1987 Documentation of Turbulence Producing Structures in Regular and Manipulated Boundary Layers. Proceedings of the IUTAM Meeting on Turbulence Control, Bangalore, India.